JOURNAL OF Materials CHEMISTRY

Effect of carburising agent on the structure of molybdenum carbides

Tiancun Xiao,[a] Andrew P. E. York,[a] Karl S. Coleman,[a] John B. Claridge,[a] Jeremy Sloan,[a] John Charnock[b] and Malcolm L. H. Green*[a]

[a]*Wolfson Catalysis Centre, Inorganic Chemistry Laboratory, University of Oxford, South Parks Road, Oxford, UK OX1 3QR. E-mail: malcolm.green@chem.ox.ac.uk; Fax: +44-1865-272690; Tel: +44-1865-272649*
[b]*CCLRC Daresbury Laboratory, Daresbury, Warrington, Cheshire, UK WA4 4AD*

Received 4th May 2001, Accepted 5th September 2001
First published as an Advance Article on the web 31st October 2001

Molybdenum carbides have been prepared by the temperature programmed reaction method using mixtures of hydrogen and methane, hydrogen and ethane, and hydrogen and butane, and characterised with X-ray diffraction, transmission electron microscopy, ^{13}C solid state NMR and EXAFS spectroscopy. The results show that the choice of hydrocarbon used to synthesise molybdenum carbide significantly affects the structure and texture of the resultant materials. Increasing the chain length of the carburising agent reduces the particle size and the temperature for complete phase transformation from molybdenum oxide to carbide is lowered. Carburising with a mixture of hydrogen and methane gives rise to hexagonal closed packed (hcp) carbide, while when using butane as the carbon source, molybdenum oxide is mainly reduced to face centred cubic (fcc) carbide. However, using ethane as the carbon source, the resultant carbide has a mixed phase composition with the hcp phase predominant. The molybdenum carbide prepared with ethane as the carbon source has the roughest surface and highest hydrogen adsorption capacity, while that prepared with butane has a very condensed surface. There is a substantial difference in the molybdenum co-ordination environments present among the carbides prepared with different carburising agents.

Introduction

High surface area transition metal carbides and oxycarbides have been found to be very active catalysts for hydrotreatment, hydrogenation, Fischer–Tropsch synthesis, hydrocarbon isomerisation, and methane reforming.[1–9] These materials have electronic and catalytic properties similar to the noble metals, but are more resistant to poisons such as sulfur and to sintering, leading them to be potential substitutes for the expensive and scarce noble metals. Also, the structure of the carbide catalyst can be tailored by changing the preparation procedures and conditions.[10–12] The structures and properties of different molybdenum carbide and oxide materials have been studied and described.[13] To date, the transition metal carbide materials are rarely used in industrial applications, as more work is needed to improve the surface area of the bulk carbides and to develop new methods to prepare supported carbide catalysts. The synthesis of these materials has attracted considerable attention over the last fifteen years and a number of routes have been developed, of which temperature programmed reaction (TPRe) of the metal oxide with methane has been the most common.[1–12,14–19] Relatively few studies have been carried out on the preparation of molybdenum carbide with other carbon sources.[17,18] Particularly amongst the hydrocarbons, there are a myriad of possible carbon sources for carburisation. Some reports have shown that replacement of methane by ethane for TPRe can lead to a higher surface area and the formation of carbide at lower temperatures.[14,15] Herein, we report the effect of the choice of carbon source for carburisation on the structure and catalytic activity of molybdenum carbides using methane, ethane and butane as the carbon agents.

Experimental

Carbide preparation

Molybdenum oxide (1.2 g, Alfa AR) powder was loaded between silica wool plugs into a quartz micro-reactor (i.d. 9 mm) and reduced with 20% vol. CH_4, 10% vol. C_2H_6, or 5% vol. C_4H_{10} in hydrogen with a total flow of 100 ml min^{-1} and at a rate of 1 K min^{-1} to different final temperatures, so as to study the MoO_3 complete phase transformation temperature. The final temperature was held for 1 h, and the sample was then naturally cooled in the carburising atmosphere to room temperature and passivated in flowing 1% vol. O_2 in He before exposure to air. The passivated carbides prepared with methane, ethane, and butane are designated as MoC-M, MoC-E, and MoC-B, respectively.

Characterisation

The XRD patterns of the molybdenum carbides were obtained using a Philips PW1710 diffractometer with Cu-Kα radiation. The carbide samples were mounted on an aluminium plate with a groove cut into it and smoothed using a microscope slide. The surface area of the molybdenum carbides was measured using an ASAP 2010 (Micrometrics Instrument Corporation) *via* the N_2 adsorption method.

The morphology of the passivated samples was studied using scanning electron microscopy (SEM) on a Hitachi S-520 microscope operated at 20 kV and 40 mA. The powder sample was dispersed on the specimen stage with acetone. A JEOL 4000FX transmission electron microscope with an accelerating voltage of 400 kV was used to investigate the crystal array of the carbide material. Electron diffraction was employed to study the crystal structure of a chosen point of the carbides. Samples were ground to a fine powder and dispersed in AR grade acetone, then placed in an ultrasonic bath for 10–20 min before a drop of the suspension was placed on a carbon-coated copper grid and put in the sample holder.

^{13}C Solid state MAS NMR measurements were carried out using a CMX-200 NMR spectrometer operating at a frequency of 50.31 MHz. Typically, 20 000 scans were accumulated using a single pulse (45°), with a pulse delay of 1.0 s and a 4 kHz s^{-1} spinning speed. The spectra were recorded at room temperature using adamantane ($\delta = 29.5$) as the reference.

 DOI: 10.1039/b104011c

EXAFS spectra were measured at the CLRC in Daresbury Laboratory. The samples were lightly ground in a pestle and mortar, and packed in aluminium sample holders with Sellotape windows. Data were collected at the Mo K-edge in a liquid nitrogen-cooled cryostat, in transmission mode on station 9.2 of the Daresbury Synchrotron Radiation Source, operating at 2 GeV with a current of between 140 and 200 mA. The Si(220) double crystal monochromator was detuned to reject 50% of the incident signal in order to minimise harmonic contamination. The monochromator angle was calibrated by running an edge scan for Mo foil. Two scans were recorded for each of the samples. The data were initially processed using the Daresbury program EXCALIB, to convert the monochromator angles to the corresponding X-ray energy, and the absorbance calculated as ln (I_o/I_t).

The isolated EXAFS data were analysed using EXCURV98 employing the exact spherical wave calculation, including multiple scattering where necessary.[20,21] Phase shifts were derived from *ab initio* calculations using Hedin–Lundqvist potentials and von Barth ground states.[22] Fourier transforms of the spectra were used to give an indication of the number of shells of back-scatterers surrounding the central metal, but all analyses were done by fitting a theoretical curve to the experimental K^3-weighted EXAFS spectra. The theoretical fits were obtained by adding shells of backscattering atoms around the central absorber atom and refining the Fermi energy, E_f, the absorber–scatterer distances, r_{ex}, and the Debye–Waller factors, $2\sigma^2$, in order to minimise the *R*-factor, which is the sum of the square of the residuals between the experiment and the theoretical fit. The numbers of scatters, *N*, was taken as the integer values that gave the best fits. Only those shells that gave a significant improvement in the *R*-factor when added to the model were included in the final fit. All pictures of the fits obtained are shown with the associated Fourier transforms (FTs).

Isotherms of hydrogen adsorption were measured at 300 K using the static volumetric technique. Prior to the adsorption measurement, each sample was pre-treated with 1 h reduction in a flow of hydrogen at 623 K and 2 h evacuation at a vacuum of 3×10^{-5} Torr at 573 K. The total uptake of hydrogen adsorption was measured at 300 K after the evacuation.

Results and discussion

TPRe-MS and XRD techniques were combined to study the complete phase transformation temperature from oxide to carbide using different carburising agents. The TPRe-MS results (described elsewhere[19]) show that molybdenum oxide starts to be reduced with methane at 943 K with no further changes occurring after it is reduced at 1023 K, suggesting that the carburisation of molybdenum oxide with methane was completed at this temperature. Ethane begins to reduce molybdenum oxide at 813 K, and is hydrogenolysed into methane at 863 K. A complete carburisation of MoO_3 using ethane occurred at 923 K after 1 h. However, using butane the carburisation of MoO_3 is very complex. Butane starts to undergo hydrocracking into methane and ethane when the temperature is raised to 723 K and is dehydrogenated to aromatics at 793 K. After 853 K, it was completely converted into methane, and there is no further change of the carburisation temperature. The XRD results show that molybdenum carbide is completely formed at 1023 K with 20% CH_4 in hydrogen, at 903 K with 10% C_2H_6, and at 823 K with 5% C_4H_{10} in hydrogen. These results are in agreement with the TPRe-MS results.

XRD patterns of the molybdenum carbides prepared with different carburising agents are shown in Fig. 1. MoC-M gives diffraction peaks at 34.3, 37.9, 39.5, and 52.2°, characteristic of hexagonal Mo_2C (*P*63/*mmc*). The diffraction peaks are sharp, revealing that the carbide is in a highly crystalline state. The molybdenum carbide derived from ethane (MoC-E) has weaker

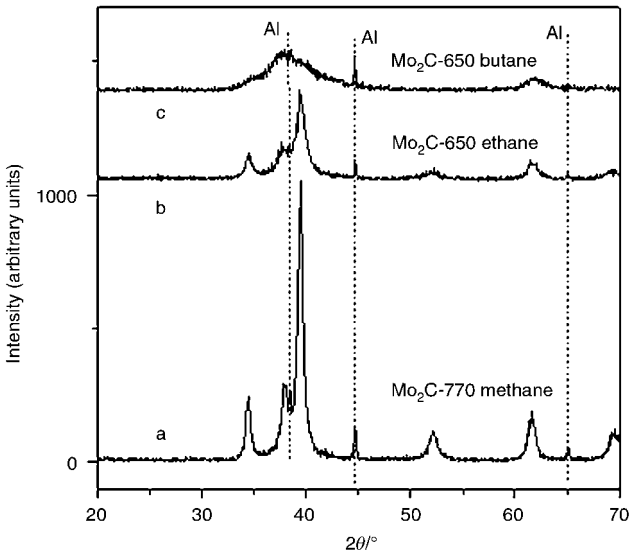

Fig. 1 XRD patterns of molybdenum carbide prepared with different carbon sources: (a) methane, (b) ethane, and (c) butane.

diffraction peaks at the same positions, indicating it has a similar structure to that of MoC-M, but the particle size is smaller. The diffraction peaks of the molybdenum carbide prepared from the carburisation using butane (MoC-B) appear at 38 and 62°. These are the characteristics peaks of the metastable η-MoC_{1-x}, which has the fcc structure. It has been pointed out that this type of molybdenum carbide can be prepared in a special process using methane, and that molybdenum carbide with the fcc structure has a similar nature and performance to that of noble metals.[23]

The temperature of the complete phase transition of MoO_3 during carburisation and the physical properties of the carbides are shown in Table 1. The particle size of molybdenum carbide decreases with the increase in carbon chain length in the carburising agent. In the XRD patterns, the full width at half maximum (FWHM) of the carbide peaks increases (particle size decreases) from methane to ethane to butane. MoC-B has the highest carbon content amongst the three samples, with the carbon content in MoC-M being the lowest. However, the atomic ratio of Mo to carbon is around 2, implying that the carbide formulas are either Mo_2C or $MoC_{0.5}$. The surface areas of MoC-M, MoC-E, and MoC-B are 30.8, 42.5, and 35.4 $m^2\ g^{-1}$, respectively.

The crystal shapes of the molybdenum carbides MoC-M, MoC-E and MoC-B, prepared using different carbon sources, were observed using scanning electron microscopy. The MoC-M crystals were found to be leaf-like with the size of the particle aggregation being about 8 μm [Fig. 2(a)]. The MoC-E is composed of small square particles, similar to that observed in its mother crystal, MoO_3 [Fig. 2(b)]. The similarity in crystal

Table 1 Complete phase transition temperature of MoO_3 carburised with different carbon sources and the composition and particle size of the prepared carbides

	Carbon source		
	CH_4	C_2H_6	C_4H_{10}
Complete phase transition temperature/K	1023	903	823
C[a]/wt%	4.98	5.03	5.72
Mo[a]/wt%	95.02	94.97	94.28
Surface area/$m^2\ g^{-1}$	30.8	42.5	35.4
Particle size[b] $r_{(220)}$/nm	5.2	3.1	1.9

[a]Chemical analysis method. [b]$D_c=0.9\lambda/(\beta\cos\theta)$, where θ refers to the 220 bond in the XRD.

shape between MoC-E and MoO_3 indicates a topotactical process during the carburisation with ethane. The scanning electron microscope image of MoC-B [Fig. 2(c)] shows a rectangular morphology, but with significant variations in particle size. MoC-B also has a similar shape to MoO_3, again suggesting a topotactical phase transition from the oxide to carbide during the carburisation. Although there is significant difference among the morphologies of the carbide particles, EDX analysis shows that the composition of the particles is almost the same.

The transmission electron microscopy (TEM) images of the molybdenum carbide produced with different carbon sources

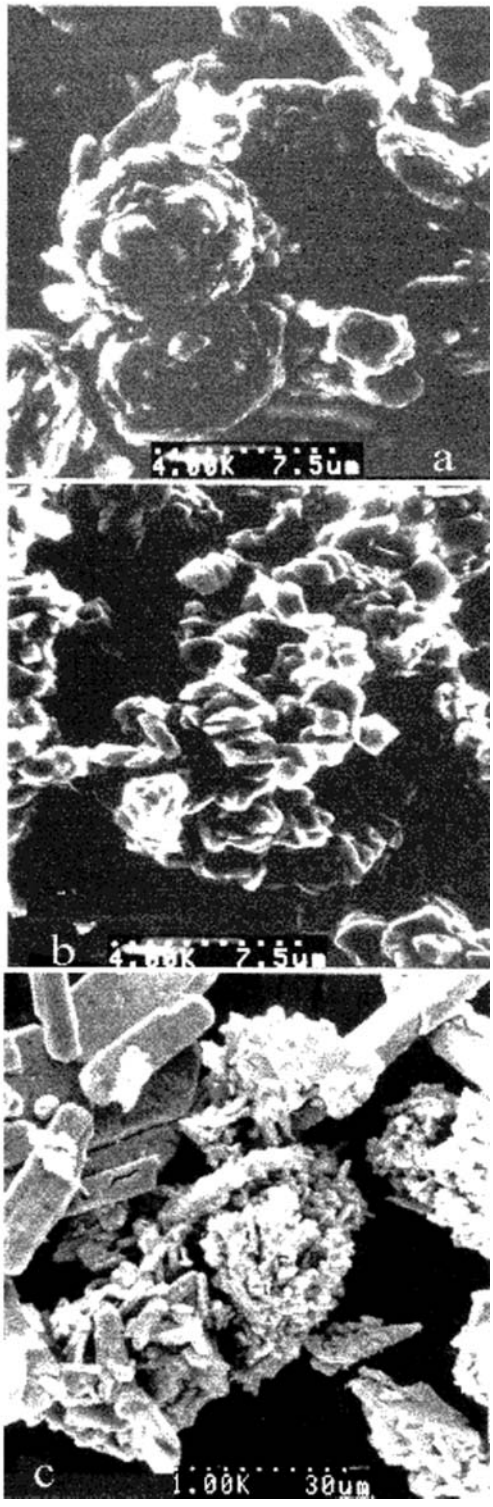

Fig. 2 SEM of the molybdenum carbide prepared with (a) methane at 1043 K, (b) ethane at 923 K, and (c) butane at 923 K.

are shown in Fig. 3. It is seen that the crystalline array of Mo_2C clearly exists in MoC-M, and the surface is rough, showing that MoC-M is a crystalline porous material, although the pore size is quite small. The surface of MoC-E is much rougher than MoC-M and is less crystalline, with the surface area larger than in the latter. This is in agreement with the XRD results. When using butane as the carbon source, the material is more condensed, with no obvious crystalline array in the material, as confirmed by the XRD results.

The electron diffraction (ED) results further support the XRD and TEM results. As shown in Fig. 4, the ED pattern of MoC-M contains a ring and dot diffraction image, suggesting that the molybdenum carbide prepared using methane consists of single crystal and polycrystalline materials. The *d*-spacing calculated from the main ring pattern is the same as that of Mo_2C, suggesting that the main phase in MoC-M is Mo_2C, although some weak ring pattern's *d*-spacing is not completely in agreement with Mo_2C. The ED pattern of MoC-E is composed of only a ring pattern, suggesting that MoC-E is a polycrystalline material; there is a clear difference between the electron diffraction patterns of MoC-M and MoC-E, suggesting that they have different phases. The ED pattern of MoC-B is the weakest, and only a few weak ring patterns are apparent, showing that the crystallinity is low. The *d*-spacing calculated from the ring pattern is the same as that of MoC_{1-x}, which further confirms that MoC-B is composed of a MoC_{1-x} phase.

The ^{13}C MAS NMR spectra of MoC-M, MoC-E and MoC-B show two bands at 113 and 273 ppm, which can be ascribed to carbon in fcc and hcp molybdenum carbide, respectively.[19] The ^{13}C NMR spectrum in Fig. 5(a) shows that MoC-M is composed of both hcp and fcc carbide. In the case of MoC-E, Fig. 5(b), the peak at 113 ppm becomes more intense, while the peak at 273 ppm decreases, suggesting that the main phase in MoC-E has the fcc structure, although there is an appreciable amount of hcp molybdenum carbide present. In MoC-B, Fig. 5(c), the peak at 273 ppm almost disappears, leaving that at 113 ppm as the main peak, suggesting that MoC-B consists mainly of fcc molybdenum carbide. These results suggested that carburisation with methane affords hcp carbide with some fcc carbide, while with ethane, mainly fcc is obtained with some hcp carbide. When using butane as the carbon source, fcc carbide is the main phase.

The EXAFS results are shown in Fig. 6 and Table 2. To optimise the analytical conditions and calibrate the results, a standard Mo_2C sample was first measured and the results compared with X-ray crystallographic data. The other prepared samples were all measured under the same conditions to guarantee the reliability of the experimental results. They further reveal the difference among the molybdenum carbides prepared with different carbon sources. In MoC-M, one molybdenum atom is surrounded with 3 carbon atoms in shell 1 with an Mo–C distance of 2.11 Å, and three Mo atoms in shell 4 with a distance of 4.27 Å, to form three linear Mo···Mo···Mo groupings. It should be noted that shell 3 comprises molybdenum scatterers at the same distance as those in shell 2, and that shell 5 comprises molybdenum scatterers at the same distance as those in shell 4. The distances derived from the EXAFS fitting agree well with the hcp molybdenum carbide (β-Mo_2C) crystal structure parameters. In MoC-E, the bond lengths are all the same as those in MoC-M, but the Debye–Waller factors for the outer shell are high. This indicates that the local structure is the same. However, there is a slight loss of order in the outer shells, implying a lower degree of crystallinity, which is in agreement with the XRD results. The EXAFS spectrum of MoC-B is in contrast with those of MoC-M and MoC-E. The intensity of the peak at 3.0 Å in the Fourier transform is much lower, the oscillations giving rise to the first Mo–C peak at 2.06 Å are best fitted with 4 carbon atoms rather than 3 or 5. The second shell is at a similar distance to those of MoC-M and MoC-E, but weaker. The shells at 3.71 and 3.98 Å

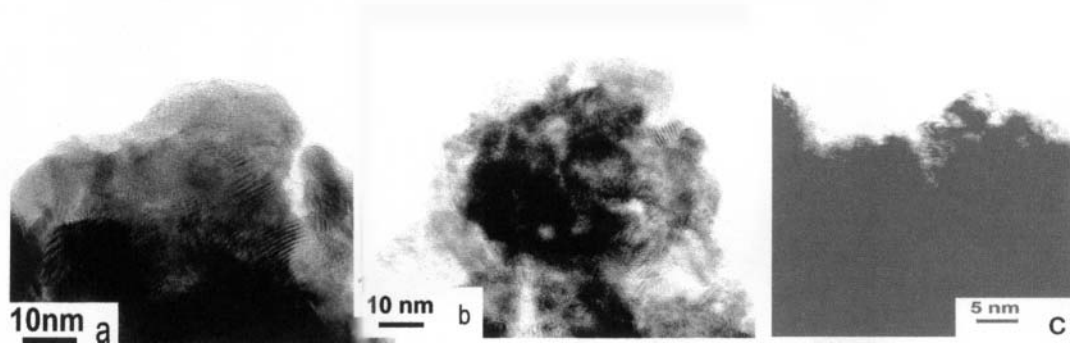

Fig. 3 TEM micrographs of molybdenum oxide carburised with (a) methane to 750 °C, (b) ethane to 650 °C, and (c) butane to 550 °C.

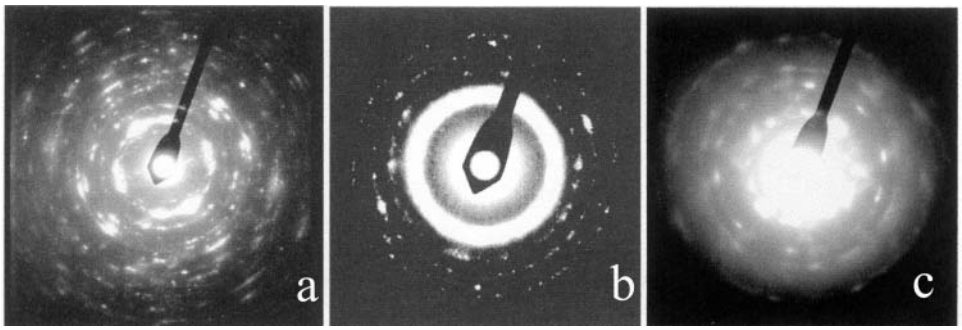

Fig. 4 Electron diffraction patterns of molybdenum carbide prepared with (a) methane, (b) ethane, and (c) butane.

are not present in this sample. Hence it is concluded that there is some crystalline molybdenum carbide, which is in the form of MoC_{1-x} with the fcc structure. As shown by the solid state NMR, this is believed to be molybdenum carbide or oxycarbide with the fcc structure.

The molybdenum carbide catalysts prepared using different carbon sources have been tested for pyridine hydrodenitrogenation (HDN)and the results are reported elsewhere.[24] MoC-E has the highest activity for pyridine HDN, and the catalyst is stable for 20 h under the reaction conditions. MoC-B is less stable and active than MoC-E, but more active than MoC-M. It is believed that molybdenum carbides having the fcc structure and a high surface area act as the active components for HDN. However, in partial oxidation of methane to synthesis

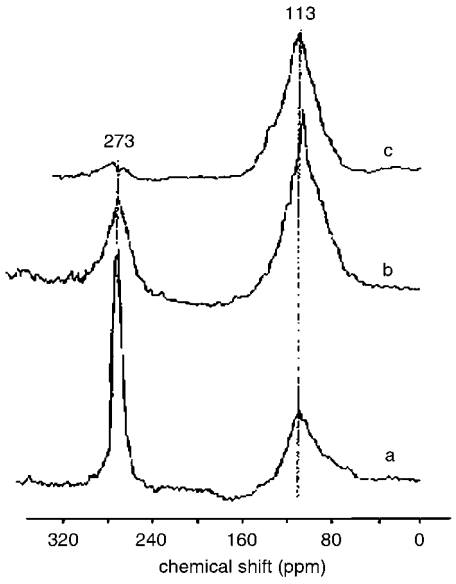

Fig. 5 ^{13}C MAS NMR spectra of the molybdenum carbides prepared from carburisation of MoO_3 with (a) methane, (b) ethane, and (c) butane.

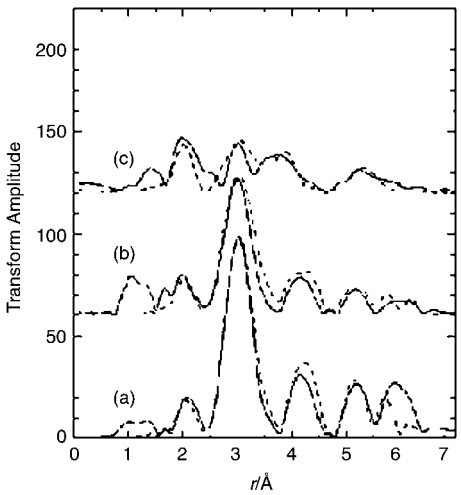

Fig. 6 Final fits of the Mo K-edge X-ray adsorption spectra of the molybdenum carbide samples: (a) MoC-M, (b) MoC-E, and (c) MoC-B.

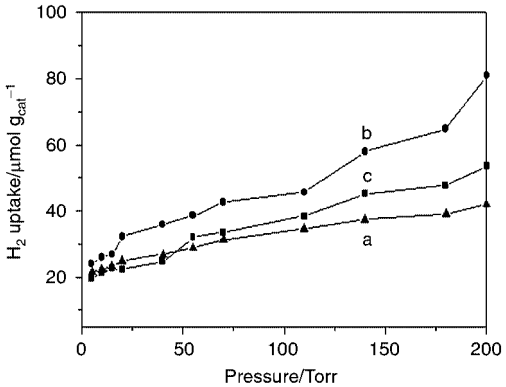

Fig. 7 H_2 adsorption isotherm over molybdenum carbides prepared with different carbon sources: (a) methane, (b) ethane, and (c) butane.

Table 2 List of final EXAFS parameters for the molybdenum carbides prepared with different carburising agents

Sample	Shell	Type	r_{ex}/Å	$2\sigma^2$/Å^2	Residual
MoC-M	1	3 × C	2.11	0.08	24.3
	2	6 × Mo	2.930	0.012	
	3	6 × Mo	3.00	0.012	
	4	3 × Mo	4.27	0.009	
	5	3 × Mo	4.27	0.009	
	6	18 × Mo	5.21	0.012	
	7	12 × Mo	5.66	0.014	
	8	6 × Mo	6.02	0.011	
MoC-E	1	3 × C	2.07	0.008	47.5
	2	6 × Mo	2.980	0.016	
	3	6 × Mo	2.98	0.016	
	4	3 × Mo	4.24	0.012	
	5	3 × Mo	4.24	0.012	
	6	18 × Mo	5.19	0.00	
	7	12 × Mo	5.69	0.017	
	8	6 × Mo	6.01	0.018	
MoC-B	1	4 × C	2.06	0.010	51.5
	2	4 × Mo	2.99	0.015	
	3	4 × Mo	3.71	0.012	
	4	4 × Mo	3.98	0.019	
	5	6 × Mo	5.20	0.012	
	6	6 × Mo	5.51	0.21	

gas, MoC-M has the highest activity and selectivity; this is because Mo_2C or Mo_3C_2 having the hcp structure is the active component.[10] The activity difference may also be due to the catalyst particle size and the hydrogen adsorption capacity. As shown in Fig. 7, MoC-E has the highest hydrogen adsorption capacity, and the amount of adsorbed hydrogen increases with the hydrogen partial pressure. This is due to the higher surface area of MoC-E, as no significant difference in hydrogen uptake per square meter is present in the three samples.

Conclusion

The temperature of the complete phase transition from molybdenum oxide to carbide decreases as the carburising agent chain becomes longer. Molybdenum carbide prepared using methane as the carbon source has mainly the hcp structure, the highest crystallinity and a leaf-like morphology. The phase transition from molybdenum oxide to carbide is topotactic. The main phase of the molybdenum carbide prepared using ethane has hcp structure, and a small amount of fcc molybdenum carbide is present. The carbide is composed of smaller square crystals. Using a mixture of hydrogen and butane to carburise molybdenum oxide leads to molybdenum carbide with fcc structure and low crystallinity. The surface of this carbide is very condensed.

Using a mixture of ethane and hydrogen as the carbon source leads to the highest surface area for the molybdenum carbide and the most stable catalyst for pyridine hydrodenitrogenation. The molybdenum carbide prepared using methane has the lowest surface area and the lowest activity and stability for pyridine HDN. The difference in HDN activity among the carbide catalysts is probably due to the structure type, crystallinity and the hydrogen adsorption capacity. The effect of the carburising agent on the structure and catalytic performance of molybdenum carbide makes it possible to design the desired catalyst by choosing a suitable alkane in the carburisation process.

Acknowledgements

T. C. X. and K. S. C. would like to thank the Royal Society for a Royal Society BP-Amoco Fellowship and a Royal Society University Research Fellowship, respectively. We wish to thank CANMET and the GRI for financial support for A. P. E. Y. and also Colebrand Ltd for support for J. B. C. We acknowledge the provision of the time on DARTS, the UK national synchrotron radiation service at the CLRC Daresbury Laboratory through funding by the EPSRC.

References

1 J. S. Lee, M. H. Yeom, K. Y. Park, I.-S. Nam, J. S. Chung, Y. G. Kim and S. H. Moon, *J. Catal.*, 1991, **128**, 126.
2 V. Schwartz, S. T. Oyama and J. G. Chen, *J. Phys. Chem. B*, 2000, **104**, 8800.
3 L. Delannoy, J.-M. Giraudon, P. Granger, L. Leclercq and G. Leclercq, *Catal. Today*, 2000, **59**, 231.
4 G. M. Dolce, P. E. Savage and L. T. Thompson, *Energy Fuels*, 1997, **11**, 668.
5 P. D. Gallo, F. Meunier, C. Pham-Huu, C. Crouzet and M. J. Ledoux, *Ind. Eng. Chem. Res.*, 1997, **36**, 4166.
6 A. P. E. York, J. B. Claridge, A. J. Brungs, S. C. Tsang and M. L. H. Green, *Chem. Commun.*, 1997, 39.
7 A. J. Brungs, A. P. E. York and M. L. H. Green, *Catal. Lett.*, 1999, **57**, 65.
8 C. Bouchy, L. Schmidt, J. R. Anderson, C. J. H. Jacoobsen, E. G. Derouane and S. B. D. Hamid, *J. Mol. Catal. A*, 2000, **163**, 283.
9 V. Schwartz, V. T. da Silva and S. T. Oyama, *J. Mol. Catal. A*, 2000, **163**, 253.
10 K. Oshikawa, M. Nagai and S. Omi, *Chem. Lett.*, 2000, **9**, 1086.
11 S. Li, L. J. Sung, T. Hyeon and K. S. Suslick, *Appl. Catal., A*, 1999, **184**, 1.
12 A. Hanif, D. Phil. Thesis, Oxford University, Oxford, UK, 2000.
13 J. G. Chen, *Chem. Rev.*, 1996, **96**, 1477.
14 M. K. Neylon, S. Choi, H. Kwon, K. E. Curry and L. T. Thompson, *Appl. Catal., A*, 1999, **183**, 253.
15 J. B. Claridge, A. P. E. York, A. J. Brungs and M. L. H. Green, *Chem. Mater.*, 2000, **12**, 132.
16 S. Z. Li, W. B. Kim and J. S. Lee, *Chem. Mater.*, 1998, **10**, 1853.
17 M. J. Ledoux, F. Meunier, B. Heinrich, C. Pham-Huu, M. E. Harlin and A. O. I. Krause, *Appl. Catal., A*, 1999, **181**, 157.
18 M. E. Harlin, A. O. I. Krause, B. Heinrich, C. Pham-Huu and M. L. Ledoux, *Appl. Catal., A*, 1999, **185**, 311.
19 T. C. Xiao, A. P. E. York, V. C. Williams, H. Al-Megren, X. Zhou and M. L. H. Green, *Chem. Mater.*, 2000, **12**, 3896.
20 P. A. Lee and J. B. Pendry, *Phys. Rev. B*, 1975, **11**, 2795.
21 S. J. Gurman, N. Binsted and I. Ross, *J. Phys. C: Solid State Phys.*, 1986, **19**, 1845.
22 L. Hedin and S. Lundqvist, *Solid State Phys.*, 1969, **23**, 1.
23 C. Bouchy, S. B. D. Hamid and E. G. Derouane, *Chem. Commun.*, 2000, 125.
24 T. C. Xiao, A. P. E. York, H. Al-Megren, J. B. Claridge, H. Wang and M. L. H. Green, *C. R. Acad. Sci., Ser. IIc: Chim.*, 2000, **3**, 451.